Nafta-Gaz 2025, no. 1, pp. 73–83, DOI: 10.18668/NG.2025.01.07

Increasing the efficiency of heat exchange by improving the design of heat exchangers

Zwiększenie wydajności wymiany ciepła poprzez ulepszenie konstrukcji wymienników ciepła

Abdugaffor M. Khurmamatov[1], Oybek Y. Ismailov[1], Alisher U. Auesbaev[1,2], Ganisher B. Rakhimov[3], Jalolidin A. Muminov[4], Zamir M. Khametov[4]

[1] *Institute of General and Inorganic Chemistry of the Academy of Sciences, Uzbekistan*
[2] *Karakhalpak State University named after Berdakh, Uzbekistan*
[3] *Karshi Engineering-Economic Institute, Uzbekistan*
[4] *Fergana Polytechnic Institute, Uzbekistan*

ABSTRACT: This article is focused on the investigation and optimization of heat exchange efficiency in a shell-and-tube heat exchanger used for heating a saturated absorbent with regenerated absorbent in the technology of purifying regeneration gas from acidic components through absorption. The optimization of heat exchange efficiency involves modifying the hydrodynamic regimes of the heat exchanger by adjusting the properties of working fluids inside the tubes and the inter-tube space. The study aims to enhance heat exchange by inducing turbulent flows inside and between the tubes. The authors examined the impact of centrifugal force on flow dynamics to improve distribution uniformity within the distribution chamber. To achieve this, a strategic reorientation of the raw material inlet nozzle in a horizontal shell-and-tube heat exchanger with a one-sided influence on the distribution chamber is proposed. Throughout the research, experiments were conducted, and heat exchange parameters were examined including flow velocity, temperature differentials, and heat transfer coefficients. The results allowed for the determination of optimal parameters to enhance heat exchange efficiency in the specific heat exchanger. This work represents a significant contribution to the heat exchange technology and can be applied to optimize processes in the oil and gas and chemical industries, as well as other sectors utilizing shell-and-tube heat exchangers. The findings advance the understanding of heat exchange mechanisms and provide practical insights for improving efficiency in various industrial applications.

Key words: heat exchangers, shell-and-tube heat exchanger, heat exchange efficiency, hydrodynamic regimes, centrifugal force, turbulent flows, absorption, fluid dynamics, optimal parameters.

STRESZCZENIE: Niniejszy artykuł poświęcony jest badaniu i optymalizacji wydajności wymiany ciepła w płaszczowo-rurowym wymienniku ciepła wykorzystywanym do ogrzewania nasyconego absorbentu z regenerowanym absorbentem w ramach technologii oczyszczania gazu regeneracyjnego z kwaśnych składników poprzez absorpcję. Optymalizacja wydajności wymiany ciepła polega na modyfikacji reżimów hydrodynamicznych wymiennika ciepła poprzez dostosowanie właściwości płynów roboczych wewnątrz rur i przestrzeni międzyrurowej. Badanie ma na celu zwiększenie wymiany ciepła poprzez indukowanie przepływów turbulentnych wewnątrz i między rurami. Autorzy zbadali wpływ siły odśrodkowej na dynamikę przepływu, celem uzyskania równomiernego rozkładu w komorze dystrybucyjnej. W tym celu zaproponowano zastosowanie strategicznego przeorientowania dyszy wlotowej surowca w poziomym płaszczowo-rurowym wymienniku ciepła przy jednostronnym wpływie na eliptyczną pokrywę otworu. W trakcie badań przeprowadzono eksperymenty i zbadano parametry wymiany ciepła, w tym prędkość przepływu, różnice temperatur i współczynniki przenikania ciepła. Wyniki pozwoliły na określenie optymalnych parametrów pozwalających na zwiększenie wydajności wymiany ciepła w konkretnym wymienniku ciepła. Praca ta stanowi znaczący wkład w technologię wymiany ciepła a jej wyniki mogą zostać wykorzystane do optymalizacji procesów w przemyśle naftowym, gazowym i chemicznym, a także w innych sektorach wykorzystujących płaszczowo-rurowe wymienniki ciepła. Wyniki badań przyczyniają się do lepszego zrozumienia mechanizmów wymiany ciepła i zapewniają praktyczny wgląd w poprawę wydajności w różnych zastosowaniach przemysłowych.

Słowa kluczowe: wymienniki ciepła, płaszczowo-rurowy wymiennik ciepła, efektywność wymiany ciepła, reżimy hydrodynamiczne, siła odśrodkowa, przepływy turbulentne, absorpcja, dynamika płynów, optymalne parametry.

Corresponding author: A. Auesbaev, e-mail: *alisherauesbaev@gmail.com*

Article contributed to the Editor: 10.05.2024. Approved for publication: 18.10.2024.

Introduction

Heat exchangers (HEs) serve as crucial heat transfer (HT) devices, enabling the exchange of thermal energy between two fluids to either cool or heat a process fluid to the desired temperature. The HT process involves conduction, radiation, and convection (Nemati and Sefid, 2022; Yeasmin et al., 2022) occurring simultaneously in practical applications. For instance, both conduction and convection takes place through a wall when cold and hot fluids interact. Typically, HT between fluids occurs without a phase change, involving convection and radiation with conduction.

Heat exchangers find widespread application across various sectors, including power plants, space heating, refineries, air-conditioning, refrigeration, food processing, chemical processing, waste heat recovery systems, automobile cooling systems, and aviation/aerospace applications. Examples of heat exchangers include evaporators, condensers, economizers, superheaters, cooling towers, and super towers used in power plants (Jankowski, 2022; Luo et al., 2022; Rashidi et al., 2022; Zolfagharnasab et al., 2022).

Heat exchangers (Gugulothu et al., 2018, 2021; Miansari et al., 2022; Auesbaev et al., 2024) are commonly employed for energy exchange in industries such as aerospace, chemical production, and refrigeration. In traditional tubular heat exchangers, the internal rigid heat transfer elements may begin to vibrate under fluid impact, potentially leading to fatigue damage and reduced service life (Gong et al., 2010; Zheng et al., 2014). Shell-and-tube heat exchangers (Gugulothu and Sanke, 2022; Gugulothu et al., 2022) currently dominate industrial applications. The study of improved heat transfer mechanisms in heat exchangers has emerged as a prominent area of current research (Nitturi et al., 2023; Ismaylov et al., 2024).

When selecting the fluids for heat exchange equipment, the following attributes are considered:
1. the degree of heating and cooling required for the environment and the ability to control it;
2. achieving a high rate of heat exchange with minimal mass and volume consumption;
3. low viscosity, high density, heat capacity, and heat of steam generation;
4. non-corrosive, non-toxic, and heat-resistant properties;
5. heat exchange equipment should not damage the prepared material;
6. affordability.

Heat exchange equipment makes up a significant portion of the technological equipment used in oil and gas refining and chemical industries. On average, heating equipment accounts for 15–18% of total equipment in the chemical industry, while in the oil and gas processing industry, it makes up around 50%. Different types of heat exchange equipment are employed in the industry, categorized by working principle into three types:
1. surface heat exchangers;
2. cooling heat exchangers;
3. regenerative heat exchangers.

Pipe furnaces widely used in the oil and gas processing industry are a separate type.

A commonly utilized industrial heat exchanger is the *Shell and Helically Coiled Heat Exchanger* (SHCTHEX), featuring helically coiled tubes within a shell. This structure induces secondary flow within the tubes due to centrifugal force, thereby enhancing heat transfer to the other fluid while occupying less space than straight tubes (Naphon, 2007; Khurmamatov et al., 2023a). Etghani and Baboli (2017) developed a model to examine the influence of certain geometric parameters, including coil diameter and pitch size, on the thermal and flow characteristics of a Shell and Helically Coiled Heat Exchanger (SHCTHEX). Similarly, Jamshidi et al. (2013) conducted experiments to analyze how coil diameter and pitch affect performance under varying flow rates, identifying optimal geometric parameters for different operating conditions.

Various methods exist to enhance the thermal performance of thermal systems such as heat exchangers (Kurian et al., 2016; Mebarek-Oudina et al., 2021; Khurmamatov and Auesbaev, 2023; Khurmamatov et al., 2023b; Shomansurov et al., 2024). A common approach involves integrating fins to increase the heat transfer surface area, thereby improving the overall heat transfer rate (Benarji et al., 2008; Afshari et al., 2019; 2021; Bianco, et al., 2021). In a study by Andrzejczyk et al. (2018), the influence of employing different types of fins and baffles on the total efficiency of a Shell and Helically Coiled Heat Exchanger (SHCTHEX) was empirically analyzed.

Another technique employed by Panahi and Zamzamian (Panahi and Zamzamian, 2017; Khurmamatov et al., 2023c) involved using a helical wire turbulator to increase turbulence intensity, thus enhancing the thermal performance of SHCTHEX. Another study conducted by Tuncer et al. (Tuncer et al., 2021; Khurmamatov et al., 2024) employed longitudinal fins to further improve heat transfer in the developed SHCTHEX. Additionally, Solanki and Kumar (2019) conducted a comparative analysis, exploring the utilization of both smooth and dimpled helically coiled tubes in SHCTHEX.

A review of the existing literature shows that various fins and baffles can enhance the thermal efficiency of Shell and Helically Coiled Heat Exchangers (SHCTHEXs). However, optimizing the overall performance of SHCTHEXs requires tailored fin and baffle modifications due to their unique design. This study focuses on improving the efficiency of SHCTHEXs by investigating how flow movement affects temperature changes during heat exchange, specifically examining the effects of circular flow movement within the distribution chamber of the SHCTHEX.

Methods and materials

To investigate the heat exchange process within gas absorption treatment technology, a shell pipe heat exchange device was assembled for research purposes. The study focused on examining the dynamic temperature variations during the process of heating rich diethanolamine using lean diethanolamine, as illustrated in Figure 1. Notably, the available literature lacks comprehensive information regarding temperature profiles during the heat exchange process, raw material consumption, and the changes in flow patterns resulting from the circular motion of the heat-carrying agent within the distribution chamber of the apparatus.

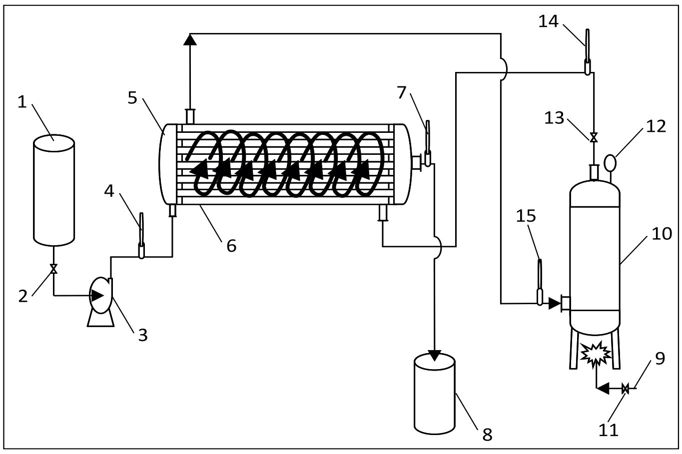

Figure 1. Technological scheme of a shell-and-tube heat exchanger with a design where flow movement in the distribution chamber is directed under the influence of centrifugal force: 1 – raw material container; 2 – raw material consumption control valve; 3 – centrifugal pump; 4, 7 – thermometers; 5 – centrifugal chamber; 6 – shell and pipe heat exchanger; 8 – high-temperature raw materials container; 9 – natural gas; 10 – gas tank; 11 – heating agent generator; 12 – pressure gauge; 13 – spring for adjusting heat carrier flow; 14, 15 – thermometers for measuring inlet and outlet temperatures of the heating agent in the shell and pipe heat exchanger

Rysunek 1. Schemat technologiczny płaszczowo-rurowego wymiennika ciepła o konstrukcji, w której ruch przepływu w komorze rozdzielczej kierowany jest pod wpływem siły odśrodkowej: 1 – zbiornik surowca; 2 – zawór regulujący zużycie surowca; 3 – pompa odśrodkowa; 4, 7 – termometry; 5 – komora odśrodkowa; 6 – płaszczowo-rurowy wymiennik ciepła; 8 – zbiornik surowca wysokotemperaturowego; 9 – gaz ziemny; 10 – zbiornik gazu; 11 – generator czynnika grzewczego; 12 – manometr; 13 – sprężyna do regulacji przepływu nośnika ciepła; 14, 15 – termometry do pomiaru temperatury wlotowej i wylotowej czynnika grzewczego w wymienniku płaszczowo-rurowym.

Following an analysis of data extracted from scientific literature and online resources, a thermal exchange apparatus was devised to systematically investigate the influence of flow movement on temperature dynamics during the heat exchange process, specifically due to the circular motion within the distribution chamber of a cubic pipe heat exchange device.

The experimental apparatus operates sequentially: the heating agent, rich diethanolamine, is introduced into the raw feed container. The raw feed is then incrementally supplied to centrifugal pump 3 with assistance from the raw material consumption control valve 2. This pump conveys the raw feed to the internal tube of the heat exchange device, which is equipped with five chambers, thereby facilitating flow circulation within the pipe heat exchanger. Subsequently, the heated raw material is directed into a collection tank.

Throughout this experimental process, the initial and final temperatures of the raw material are measured using thermometers 4 and 7, respectively. Volume consumption is determined by measuring the volume of raw material collected in the tank over a specified time period.

The experimental apparatus is characterized by a cubic pipe with a length of 2,000 mm and a diameter of 76 mm. Internally, the cubic structure accommodates five pipes with a 10 mm diameter. Experimental trials were conducted with the raw material velocity within the internal pipe ranging from 0.5 to 1.0 m/s.

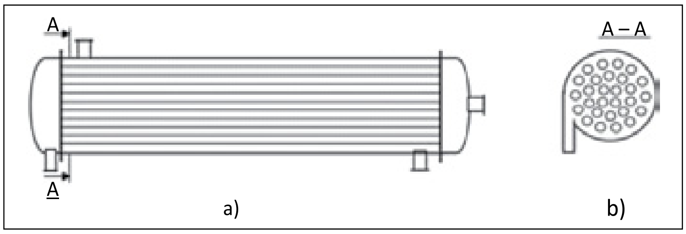

Figure 2. Shell-and-tube heat exchanger working under the influence of centrifugal force

Rysunek 2. Płaszczowo-rurowy wymiennik ciepła wykorzystujący siłę odśrodkową

The centrifugal force within the distribution chamber of the cubic pipe experiment in the heat exchange device, as illustrated in Figure 2, was computed based on the technical parameters of the experimental setup. These parameters include the dimensions and characteristics of the construction: the diameter of the upper pipe of the heat exchanger D = 72/76 mm; diameter of internal pipes d = 10/13 internal pipe length L = 1800 mm; number of internal pipes n = 5; height of the distribution chamber H = 55 mm; heat exchanger surface of experimental device F = 0.565 m^2; pipe diameter d = 20 mm for the entrance of raw materials.

In the device's distribution chamber, the mass of raw materials is determined by formula (1):

$$m = (\pi \cdot D^2/4)H \cdot \rho \tag{1}$$

where:
D – diameter of the heat exchanger shell [m],
H – height of distribution chamber [m],
ρ – density [kg/m^3].

To allow raw materials to enter the distribution chamber, the speed in the pipe is determined by the following formula:

$$\upsilon = 4 \cdot V / (3600 \cdot \pi \cdot d_p^2) \tag{2}$$

where:
d_p – diameter of the inlet pipe [m],
V – volumetric flow rate [m^3/h].

It was determined that the magnitude of the centrifugal force decreases at different radii, ranging from 0.1–0.5 percent of the internal diameter of the device's distribution chamber.

Centrifugal force magnitude is determined by formula (3), which depends on the radii of the current circulating in the distribution chamber:

$$C_1 = mv^2/R = 0.26 \cdot 0.23^2/R_1 \tag{3}$$

where:
C_1 – centrifugal force [N],
v – speed in the pipe [m/s].

The ratio of centrifugal force to rotational force (K), which determines the efficiency of raw material distribution in the internal pipes of the heat exchange device, is determined using formula (4):

$$K = \frac{C_1}{G} = \frac{\frac{m \cdot v^2}{R}}{m \cdot g} = \frac{v^2}{R \cdot g} \tag{4}$$

The amount of heat transferred along the heat exchange surface F [m^2] Q [Wt] is calculated by:

$$Q = K\,\Delta_{tave} F\tau \tag{5}$$

where:
K – overall heat transfer coefficient [Wt/(m$^2 \cdot$K)],
Δ_{tave} – thermal agent temperature difference [°C],
τ – process duration [min].

The working surface of the heat exchanger is determined by the following formula:

$$F = Q/(K \cdot \Delta_{tave}) \tag{6}$$

The overall heat transfer coefficient is determined using the following formula, taking into account the coefficients of heat transfer, the thickness of the pipe wall and its heat transfer coefficients, the flood thickness on the pipe wall, and its thermal conductivity.

$$K = \frac{1}{\frac{1}{\alpha_1} + \frac{\delta_1}{\lambda_1} + \frac{\delta_w}{\lambda_w} + \frac{1}{\alpha_2}} \tag{7}$$

where:
α_1 – individual heat transfer coefficient Wt/(m$^2 \cdot$K) given from heat carrier to pipe outer wall,
α_2 – individual heat transfer coefficient from the pipe wall to the cold current is Wt/(m^2/K);
δ_w – wall thickness,
δ_1 and δ_2 – flood thickness on the wall by hot and cold carriers [m],
λ_w – thermal conductivity of the pipe wall,
λ_1 and λ_2 – thermal conductivity of the dash on the outer and inner sides of the pipe wall [Wt/(m$\cdot$K)].

Results and discussions

Throughout the investigation conducted with the shell-and-tube experimental device, various parameters were systematically measured and are detailed in Table 1. These parameters include the rotational rate within the distribution chamber of raw materials, denoted as R_1(0.1D), which covers the degrees in the range of R_5(0.5D), the magnitude of centrifugal force denoted as C in [Pascals], the percentage increase in centrifugal force, j_c [%], and the efficiency of raw material distribution within the pipe, K [%].

Analysis of the data in Table 1 reveals a significant improvement in the degree of raw material supply to internal pipes, registering an additional increment of 7.4% under the influence of centrifugal force-induced flow movement within the distribution chamber of the device. Consequently, this normalization of the distribution of the heat from the heating agent leads to an improvement in thermal efficiency. At the

Table 1. Production process efficiency of raw material distribution in the inner pipe of the heat exchanger with a hollow pipe under the influence of centrifugal force

Tabela 1. Efektywność procesu dystrybucji surowca w wewnętrznej rurze wymiennika ciepła z rurą drążoną pod wpływem siły odśrodkowej

Centrifugal force	Work of rotation of centrifugal force in the raw material distribution chamber				
	R_1 (0.1·D)	R_2 (0.2·D)	R_3 (0.3·D)	R_4 (0.4·D)	R_5 (0.5·D)
Magnitude of centrifugal force, C [Pa]	1900	951	634	475	380
Increase of centrifugal force, j_c [%]	100	50.0	33.6	25.0	–
Raw material distribution efficiency in the pipeline, K [%]	7.4	3.7	2.4	1.8	1.4

same time, a slowing down of the process of creating a flow on the inner surface of the pipe is observed.

In the course of the experimental procedure, outcomes of heating rich diethanolamine with lean diethanolamine in a shell-and-tube heat exchange device were discerned and systematically documented, as presented in Table 2.

The data presented in Table 2 indicates that the temperature of the heating agent (rich diethanolamine) upon entering the inner pipe of the shell-and-tube device is t_1 = 25°C, while the temperature of the heating agent (lean diethanolamine) at the exit from the heating boiler is t_4 = 108°C. Within this temperature range, the temperature variation of the heated raw material was observed at different consumption rates (V = 1–5 l/min).

Table 2. Dependence of flow temperature in the cubic pipe heat exchanger on the raw material flow rate

Tabela 2. Zależność temperatury przepływu w płaszczowo--rurowym wymienniku ciepła od natężenia przepływu surowca

Raw material consumption, V [l/min]	Temperature of heated substance [°C]		Heating agent temperature [°C]	
	t_1	t_2	t_3	t_4
1	25	87	108	81
2	25	85	108	82
3	25	82	108	84
4	25	78	108	86
5	25	71	108	89

Specifically, when the consumption of the raw material being heated was set at 1 l/min, an increase in temperature from t_1 = 25°C to 87°C resulted in a decrease in the heating agent temperature from t_3 = 108°C to 81°C. Conversely, increasing raw material consumption to 5 l/min resulted in an increase in the heating agent temperature to t_2 = 71°C, causing the heating agent temperature to drop to t_4 = 89°C.

The results indicate that an increase in raw material consumption from 1 l/min to 5 l/min results in a decline in the temperature of the heated agent by 16°C, while the total volume of heated raw materials experiences a fivefold increase.

Table 3 presents the experimental results of the process of heating rich amine with lean amine. Experiments were conducted in conditions where the pressure of the heating agent was P = 50–200 kPa, and the raw material consumption was V = 1–10 l/min.

Throughout the heating process, the pressure of the heating agent (P) ranged from 50 to 200 kPa, while the pressure of the heat source (V) varied between 1 and 5 l/min. The temperature of the heating agent (rich amine) at the exit from the heating cauldron exceeded the range of t_1 = 86–114°C, correspond-

Table 3. Temperature dependence of heating of rich amine with lean amine (heating agent pressure: 50–200 kPa)

Tabela 3. Zależność nagrzewania aminy wzbogaconej za pomocą aminy ubogiej

Pressure of heating agent	Raw material consumption, V	Lean amine temperature at pipe		Rich amine temperature at pipe	
		inlet, t_1	exit, t_2	inlet, t_3	exit, t_4
[kPa]	[l/min]	[°C]		[°C]	
50	1	88	46	20	67
	3	88	45	20	64
	5	87	45	20	63
	7	86	44	20	62
	10	86	44	20	60
100	1	103	68	20	89
	3	103	66	20	86
	5	103	64	20	82
	7	103	62	20	81
	10	103	60	20	78
150	1	106	72	20	91
	3	105	71	20	89
	5	105	69	20	86
	7	105	67	20	83
	10	105	65	20	80
200	1	114	76	20	94
	3	113	74	20	91
	5	113	71	20	88
	7	112	69	20	85
	10	110	68	20	80

ing to variations in the transmitted pressure in the range of P = 50–200 kPa. Subsequently, the temperature of the heating agent at the exit from the heat exchanger was recorded as t_2 = 45–76°C. The temperature of the rich amine, normalized to the initial temperature t_3 = 20°C and corresponding to a change in volume ratio V = 1–10 l/min, was determined from experimental observations as t_4 = 60–94°C.

A variation in raw material consumption within the range of V = 1–10 l/min results in an increased flow rate of the raw material being heated within the internal pipes of the heat exchanger. Additionally, it is evident that increasing the pressure of the heating agent in the device shell (P = 50–200 kPa) correlates with an increased average temperature within the device, denoted as Δt [°C]. Specifically, at a pressure of 50 kPa, the average temperature ranges between 23.5–24°C. This average temperature increases to 31–32.5°C at 100 kPa, 33–35°C at 150 kPa, and 38–39°C at 200 kPa. Consequently, it is observed that increasing the pressure of the heating agent, along with the raw material flow rate, induces chaotic movement of the liquid within the pipes, thereby accelerating the heat exchange process within the device.

Heat indicators of the process of heating sulfur-saturated diethanolamine with lean amine in a shell pipe heat exchanger are presented in Tables 4–7. Table 4 shows that as a result of the increase in the feedstock speed in the internal pipes of the heat exchanger from 0.017 to 0.176 m/s, the average temperature difference of the heat agent increased from zero Δt_{av} = 23.5 to 25°C. The Reynolds criterion increased from 218 to 2,298, shifting from laminar to turbulent mode. The individual coefficient of heat transfer varies between α_2 = 179 to 681 Wt/(m$^2 \cdot$K), and the overall heat transfer coefficient (K) from 165 to 681 Wt/(m$^2 \cdot$K), the amount of heat increased from Q = 2,191 to 7,319 W.

When the temperature of the lean amine was 103°C and the pressure was 100 kPa, the raw material heating rate in the pipe increased from 0.017 to 0.176 m/s. As a result, the temperature fluctuated from 89°C to 78°C, the Reynolds number incresaed 10 times, the individual heat transfer coefficient increased 3.5 times, the overall heat transfer coefficient increased 3.0 times, and the heat amount increased 3.2 times.

When the temperature of the heating agent was 105°C and the pressure was 150 kPa, the temperature of the raw material being heated varied from 91 to 80°C as flow rate increased. The mean temperature difference rose from 33.5 to 35°C. The Reynolds criterion increased from 258 to 2587, shifting from laminar to turbulent mode. The individual heat transfer coefficient increased from 212 to 814 Wt/(m$^2 \cdot$K), while the overall heat transfer coefficient increased from 198 to 645 Wt/(m$^2 \cdot$K), and the amount of heat increased from 3,748 to 12,759 Wt.

It was found that the temperature of the raw material being heated increased from 20°C to 94°C when the tempera-

Table 4. Heat indicators of rich amine (lean amine temperature 88°C, pressure 50 kPa)

Tabela 4. Wskaźniki ciepła aminy wzbogaconej (temperatura aminy ubogiej 88°C, ciśnienie 50 kPa)

Speed of raw material in internal pipes, ω	Raw material input temperature, t_{in}	Raw material output temperature, t_{out}	Reynolds criterion, Re	Individual heat transfer coefficient, α_2	Overall heat transfer coefficient, K	Average temperature difference of the heating agent, Δt_{av}	Amount of heat, Q
[m/s]	[°C]	[°C]		[Wt/(m$^2 \cdot$K)]	[Wt/(m$^2 \cdot$K)]	[°C]	[Wt]
0.017	20	67	218	179	165	23.5	2191
0.053	20	64	724	312	272	24.5	3766
0.088	20	63	1186	461	380	24.5	5262
0.124	20	62	1645	513	414	24.5	5732
0.176	20	60	2298	681	518	25.0	7319

Table 5. Heat indicators of rich amine (lean amine temperature 103°C, pressure 100 kPa)

Tabela 5. Wskaźniki ciepła aminy wzbogaconej (temperatura aminy ubogiej 103°C, ciśnienie 100 kPa)

Speed of raw material in internal pipes, ω	Raw material input temperature, t_{in}	Raw material output temperature, t_{out}	Reynolds criterion, Re	Individual heat transfer coefficient, α_2	Overall heat transfer coefficient, K	Average temperature difference of the heating agent, Δt_{av}	Amount of heat, Q
[m/s]	[°C]	[°C]		[Wt/(m$^2 \cdot$K)]	[Wt/(m$^2 \cdot$K)]	[°C]	[Wt]
0.017	20	89	242	198	185	31.0	3 241
0.053	20	86	754	354	314	31,5	5 590
0.088	20	82	1253	489	417	32.0	7 542
0.124	20	81	1766	574	477	32,5	8 762
0.176	20	78	2507	703	563	32,5	10 341

Table 6. Heat indicators of rich amine (lean amine temperature 105°C, pressure 150 kPa)
Tabela 6. Wskaźniki ciepła aminy wzbogaconej (temperatura aminy ubogiej 105°C, ciśnienie 150 kPa)

Speed of raw material in internal pipes, ω	Raw material input temperature, t_{in}	Raw material output temperature, t_{out}	Reynolds criterion, Re	Individual heat transfer coefficient, α_2	Overall heat transfer coefficient, K	Average temperature difference of the heating agent, Δt_{av}	Amount of heat, Q
[m/s]	[°C]	[°C]		[Wt/(m²·K)]	[Wt/(m²·K)]	[°C]	[Wt]
0.017	20	91	258	212	198	33.5	3 748
0.053	20	89	763	397	352	33.5	6 664
0.088	20	86	1294	543	462	34,0	8 878
0.124	20	83	1821	668	550	34.5	10 724
0.176	20	80	2587	814	645	35,0	12 759

Table 7. Heat indicators of rich amine (lean amine temperature 114°C, pressure 200 kPa)
Tabela 7. Wskaźniki ciepła aminy wzbogaconej (temperatura aminy ubogiej 114°C, ciśnienie 200 kPa)

Speed of raw material in internal pipes, ω	Raw material input temperature, t_{in}	Raw material output temperature, t_{out}	Reynolds criterion, Re	Individual heat transfer coefficient, α_2	Overall heat transfer coefficient, K	Average temperature difference of the heating agent, Δt_{av}	Amount of heat, Q
[m/s]	[°C]	[°C]		[Wt/(m²·K)]	[Wt/(m²·K)]	[°C]	[Wt]
0,017	20	94	282	268	248	38	5 326
0,053	20	91	803	425	378	38	8 118
0,088	20	88	1426	617	522	38	11 211
0,124	20	85	2031	748	613	38	13 165
0,176	20	80	2869	916	722	39	15 914

ture of the regenerated diethanolamine entering the device reached 114°C and the pressure was 200 kPa. Increasing raw material speed in internal pipes from 0.017 m/s to 0.176 m/s led to a tenfold increase in the Reynolds number, a 3.4-fold increase in the individual heat transfer coefficient, a 2.9 fold increase in the overall heat transfer coefficient, and a threefold increase in the amount of heat.

Further experiments examined the effects of temperature, pressure, and changes in the rate at which raw materials are heated in the heat exchanger on the amount of heat (Figure 3).

According to Figure 3, when the temperature of the heating agent (regenerated diethanolamine) was 88°C and the pressure was 50 kPa, as a result of the change in the speed of the raw material (lean amine) being heated in the internal pipes (0.017–0.176 M/s), the amount of heat increased in the range of 2191–7319 W (3.3 times). When the temperature of the heating agent was 103°C and the pressure was 100 kPa, the amount of heat increased from 3,241 to 10,341 Wt (3.2 times). When the temperature of the heat agent was 105°C and the pressure was 150 kPa, the amount of heat increased from 3748 to 12,759 Wt. Increasing the temperature to 114°C and the pressure to 200 kPa increased the amount of heat from 5,326 to 15,914 Wt (2.9 times).

In general, increasing the temperature of the heating agent and the speed of the raw material in the pipes led to an average

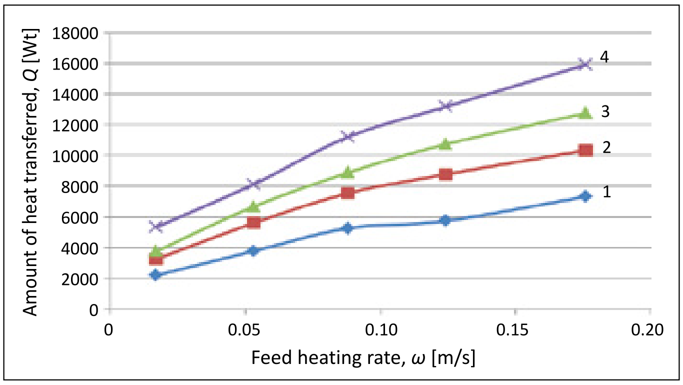

Figure 3. The effects of temperature, pressure of the heat agent, and changes in the rate at which raw materials are heated on the amount of heat:
1 – heating agent temperature 88°C and pressure 50 kPa;
2 – heating agent temperature 103°C and pressure 100 kPa;
3 – heating agent temperature 105°C and pressure 150 kPa;
4 – heating agent temperature 114°C and pressure 200 kPa

Rysunek 3. Wpływ temperatury, ciśnienia czynnika grzewczego oraz zmian szybkości ogrzewania surowców na ilość ciepła:
1 – temperatura czynnika grzewczego 88°C i ciśnienie 50 kPa;
2 – temperatura czynnika grzewczego 103°C i ciśnienie 100 kPa;
3 – temperatura czynnika grzewczego 105°C i ciśnienie 150 kPa;
4 – temperatura czynnika grzewczego 114°C i ciśnienie 200 kPa

7.2-fold increase in the amount of heat. A number of experimental and computational studies have been carried out and graphs prepared with the aim of improving the efficiency of heat exchangers, including:

- the effect of pressure changes within the shell on the individual heat transfer coefficient and overall heat transfer coefficient (Figure 4);
- the effect heating agent temperature change on the Reynolds criterion (Figure 5);
- the dependence of raw material temperature at the exit from the device on the difference in average temperatures (Figure 6);
- the effect of heating agent temperature change on the individual heat transfer and overall heat transfer coefficient (Figure 7).

Figure 4 shows that increasing the pressure of the heating agent in the shell of the device from 50 kPa to 200 kPa led to an increase in the individual coefficient of heat transfer to the raw material being heated through the inner pipe wall from 179 to 268 Wt/(m^2·K) (a 1.5-fold increase). At the same time, the overall heat transfer coefficient rose from 165 to 248 Wt/(m^2·K) (a 1.5-fold increase).

As shown in Figure 5, when the temperature of the heat agent was 88°C, the Reynolds criterion for the flow of raw materials being heated was 2,298. With an increase in temperature to 103°C, the Reynolds criterion rose to 2,507; at 105°C, it increased to 2,587; and when the temperature reached 114°C, the Reynolds criterion rose to 2,869. This leads to an increase in heat transfer coefficient, facilitating a transition in the flow regime.

Figure 6 shows that the average temperature difference of the heating agent increases from 23.5°C to 38°C as the temperature of the heated raw material at the exit from the device increase from 67°C to 94°C. An increase in the difference in average temperatures is considered the primary factor contributing to an increase in the heat transfer coefficient.

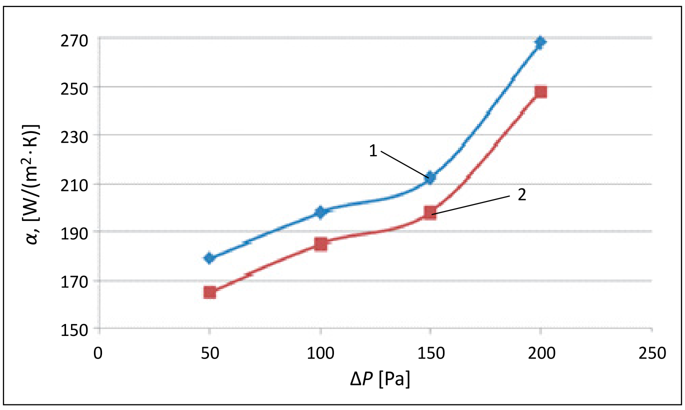

Figure 4. Effect of pressure change on the individual heat transfer coefficient α_2 and overall heat transfer coefficient K: 1 – individual heat transfer coefficient, α_2; 2 – overall heat transfer coefficient, K

Rysunek 4. Wpływ zmiany ciśnienia na indywidualny współczynnik przenikania ciepła α_2 i całkowity współczynnik przenikania ciepła K: 1 – indywidualny współczynnik przenikania ciepła α_2; 2 – całkowity współczynnik przenikania ciepła K

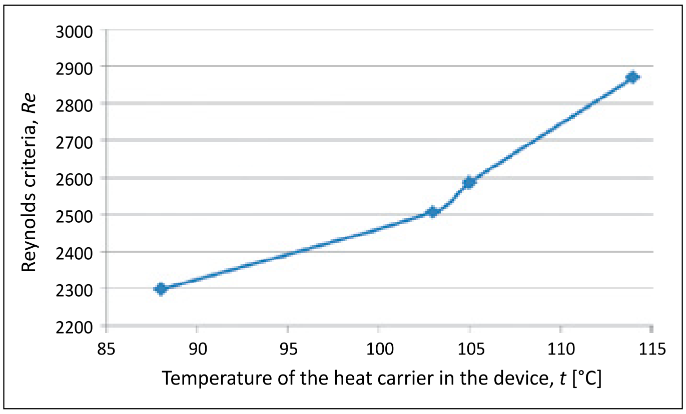

Figure 5. The effect of heating agent temperature change on the Reynolds criterion

Rysunek 5. Wpływ zmiany temperatury czynnika grzewczego na kryterium Reynoldsa

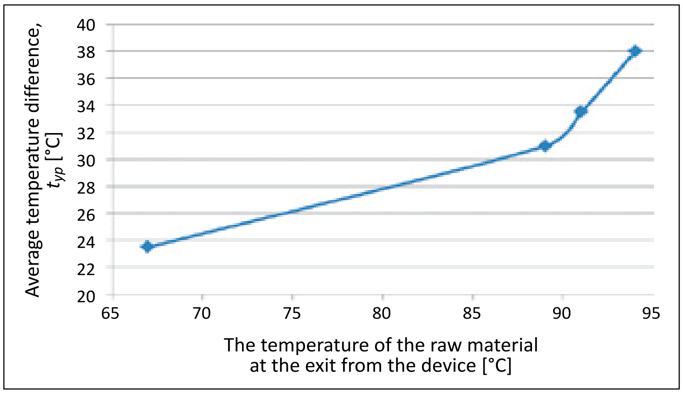

Figure 6. The dependence of the temperature of the raw material at the exit from the device on the difference in average temperatures

Rysunek 6. Zależność temperatury surowca na wyjściu z urządzenia od różnicy średnich temperatur

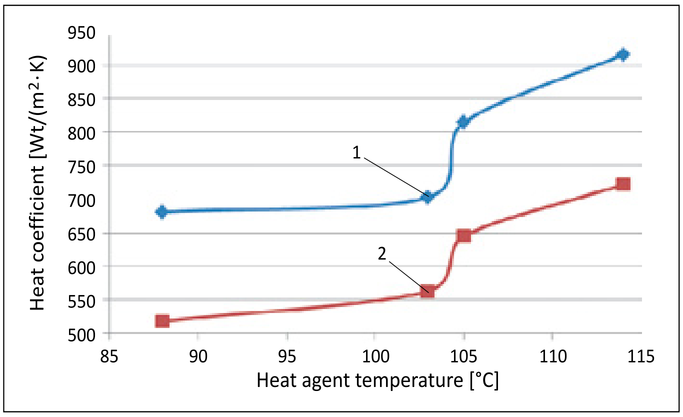

Figure 7. The effect of the change in the temperature of the heating agent on the individual heat transfer coefficient α_2 and overall heat transfer coefficient K: 1 – individual heat transfer coefficient, α_2; 2 – overall heat transfer coefficient, K

Rysunek 7. Wpływ zmiany temperatury na indywidualny współczynnik przenikania ciepła α_2 i całkowity współczynnik przenikania ciepła K: 1 – indywidualny współczynnik przenikania ciepła α_2; 2 – całkowity współczynnik przenikania ciepła K

Figure 7 illustrates the effect of changing the temperature of the heating agent on the individual heat transfer coefficient (α_2) and overall heat transfer coefficient K. When the heating agent temperature was 88°C, the individual heat transfer coefficient was 681 Wt/(m$^2\cdot$K), and the overall heat transfer coefficient was 518 Wt/(m^2 K). At 114°C, α_2 = 916 Wt/(m$^2\cdot$K), K = 722 Wt/(m$^2\cdot$K), representing a 1.34-fold and 1.39-fold increase, respectively.

Summarizing the results, an increase in the heating agent temperature at the entrance to the heat exchanger from 88°C to 114°C results in an increase in the pressure in the shell of the device from 50 kPa to 200 kPa. As a result of increasing the flow rate of the raw material being heated in the pipe from 0.017 m/s to 0.176 m/s, the temperature increased from 60°C to 94°C. This led to a 11.8-fold increase in the Reynolds number, a 5.11-fold increase in the individual coefficient of heat transfer to the raw material being heated, a 4.3-fold increase in the overall heat transfer coefficient, and a 7.2-fold increase in the amount of heat.

This study aims to enhance heat exchange efficiency in a shell-and-tube heat exchanger employed in the process of heating saturated absorbent with regenerated absorbent in the technology of regeneration gas purification from acidic components using the absorption method. The strategy involves optimizing heat exchange efficiency by modifying the hydrodynamic regimes of the heat exchanger through alterations in the agents within the internal pipes and inter-tube space.

Efficient heat exchange is achieved by inducing turbulent flow patterns within the internal pipes and inter-tube space. The article explores the manipulation of centrifugal force on flow dynamics, aiming to enhance distribution within the distribution chamber by strategically orienting the inlet nozzle for raw materials in a one-way horizontal shell-and-tube heat exchanger to impact the distribution chamber.

Conclusion

In conclusion, this research provides valuable insights into improving heat exchange efficiency in gas absorption treatment technology. The designed experimental apparatus, utilizing a cubic pipe heat exchange device, enabled systematic investigation of the effects of flow movement on temperature dynamics during the heat exchange process. Notably, the findings emphasize the significance of centrifugal force-induced flow patterns in enhancing heat distribution within the device.

The results of various experiments, including sulfur-rich amine soaking with regenerated diethanolamine, shed light on the intricate interplay between temperature, pressure, and raw material consumption. The observed increase in transferred heat, heat supply coefficient, and heat transfer coefficient underlines the practical implications of optimizing operating parameters.

Beyond theoretical considerations, this study offers practical insights for industrial applications. The proposed modifications to the hydrodynamic regimes of heat exchangers, especially the shell-and-tube heat exchanger, provide a way to improve overall system efficiency. The strategic placement of the inlet nozzle exemplifies a tangible approach to harnessing centrifugal force for improved heat distribution.

In essence, this research contributes to a broader understanding of heat exchange mechanisms and provides concrete recommendations for optimizing heat exchanger design, particularly in applications involving gas purification and regeneration gas treatment. Future work could explore additional geometric and operational optimizations to further refine the efficiency of heat exchange processes in industrial settings.

References

Afshari F., Sozen A., Khanlari A., Tuncer A.D., 2021. Heat transfer enhancement of finned shell and pipe heat exchanger using Fe_2O_3/water nanofluid. *Journal of Central South University*, 28(11): 3297–3309. DOI: 10.1007/s11771-021-4856-x.

Afshari F., Zavaragh H.G., Di Nicola G., 2019. Numerical analysis of ball-type turbulators in pipe heat exchangers with computational fluid dynamic simulations. *International Journal of Environmental Science and Technology*, 16(5): 3771–3780. DOI: 10.1007/s13762-018-2012-4.

Andrzejczyk R., Muszynski T., Gosz M., 2018. Experimental investigations on heat transfer enhancement in shell coil heat exchanger with variable baffles geometry. *Chemical Engineering and Processing – Process Intensification*, 132: 114–126. DOI: 10.1016/j.cep.2018.08.017.

Auesbaev A.U., Khurmamatov A.M., Ismaylov O.Y., Khametov Z.M., 2024. Study of the thickness of the boundary layer of hydrocarbons in horizontal tubes of heat exchangers. *Processes of Petrochemistry and oil refining*, 25(3): 931–941.

Benarji N., Balaji C., Venkateshan S.P., 2008. Optimum design of cross-flow shell and pipe heat exchangers with low fin tubes. *Heat Transfer Engineering*, 29(10): 864–872. DOI: 10.1080/01457630802125724.

Bianco N., Iasiello M., Mauro G.M., Pagano L., 2021. Multi-objective optimization of finned metal foam heat sinks: tradeoff between heat transfer and pressure drop. *Applied Thermal Engineering*, 182: 116058. DOI: 10.1016/j.applthermaleng.2020.116058.

Etghani M.M., Baboli S.A.H., 2017. Numerical investigation and optimization of heat transfer and exergy loss in shell and helical pipe heat exchanger. *Applied Thermal Engineering*, 121: 294–301. DOI: 10.1016/j.applthermaleng.2017.04.074.

Gong Y., Zhong J., Yang Z.G., 2010. Failure analysis of bursting on the inner pipe of a jacketed pipe in a tubular heat exchanger. *Materials & Design*, 88: 4258–4268. DOI: 10.1016/j.matdes.2010.04.010.

Gugulothu R., Sanke N., 2022. Use of segmental baffle in shell and pipe heat exchanger for nano emulsions. *Heat Transfer*, 51: 2645–2666. DOI: 10.1002/htj.22418.

Gugulothu R., Sanke N., Ahmed F., Jilugu R.K., 2021. Numerical study on shell and pipe heat exchanger with segmental baffle. *Proceedings of International Joint Conference on Advances in Computational Intelligence*, 309–318. DOI: 10.1007/978-981-16-0586-4_25.

Gugulothu R., Sanke N., Gupta A.V.S.S.K.S., 2018. Numerical study of heat transfer characteristics in shell-and-tube heat exchanger. *Numerical Heat Transfer and Fluid Flow*, 375–383. DOI: 10.1007/978-981-13-1903-7_43.

Gugulothu R., Sanke N., Nagadesi S., Jilugu R.K., 2022. Thermal hydraulic performance of helical baffle shell and pipe heat exchanger using RSM method. *Applied Analysis, Computation and Mathematical Modelling in Engineering*, 1: 167–187. DOI: 10.1007/978-981-19-1824-7_11.

Ismaylov O.Y., Khurmamatov A.M., Ismaylov M.K., Auesbaev A.U., Utegenov U.A., 2024. Investigations of the impact of the magnetic field on the process of formation of scaling in thermal devices. *Nafta-Gaz*, 80(2): 115–121. DOI: 10.18668/NG.2024.02.07.

Jamshidi N., Farhadi M., Ganji D.D., Sedighi K., 2013. Experimental analysis of heat transfer enhancement in shell and helical pipe heat exchangers. *Applied Thermal Engineering*, 51(1): 644–652. DOI: 10.1016/j.applthermaleng.2012.10.008.

Jankowski M., 2022. A new indicator for minimizing size of an ORC power plant based on heat exchanger and turbine design parameters. *Applied Thermal Engineering*, 201(A): 117750, DOI: 10.1016/j.applthermaleng.2021.117750.

Khurmamatov A.M., Auesbaev A.U., 2023. Analysis of the operating mode of the existing desorber and its modernization using additional contact devices. *Nafta-Gaz*, 79(6): 412–419. DOI: 10.18668/NG.2023.06.05.

Khurmamatov A.M., Auesbaev A.U., Ismaylov O.Y., Begzhanova G.B., 2023a. Effect of temperature on the physico-chemical properties of n-methyldiethanolamine. *Processes of Petrochemistry and Oil Refining*, 24(1): 99–107.

Khurmamatov A.M., Matkarimov A.M., Auesbaev A.U., Utegenov U.A., 2023b. Results of experiments on studying the composition and purification of technical water of oil and gas processing plant. *Processes of Petrochemistry and oil refining*, 24(4): 671–678.

Khurmamatov A.M., Yusupova N.K., Auesbaev A.U., Abdurakhimov S.S., 2023c. Results of a study on the treatment and separation of water from hydrocarbon waste. *Processes of Petrochemistry and oil refining*, 24(3): 421–430.

Khurmamatov A.M., Yusupova N.K., Auesbaev A.U., 2024. Possibilities for producing secondary materials from hydrocarbon waste. *Nafta-Gaz*, 11: 723–728. DOI: 10.18668/NG.2024.11.07

Kurian R., Balaji C., Venkateshan S.P., 2016. Experimental investigation of near compact wire mesh heat exchangers. *Applied Thermal Engineering*, 108: 1158–1167. DOI: 10.1016/j.applthermaleng.2016.07.172.

Luo D., Sun Z., Wang R., 2022. Performance investigation of a thermoelectric generator system applied in automobile exhaust waste heat recovery. *Energy*, 238(B): 121816, DOI: 10.1016/j.energy.2021.121816.

Mebarek-Oudina F., Fares R., Aissa A., Lewis R.W., Abu-Hamdeh N.H., 2021. Entropy and convection effect on magnetized hybrid nano-liquid flow inside a trapezoidal cavity with zigzagged wall. *International Communications in Heat and Mass Transfer*, 125: 105279. DOI: 10.1016/j.icheatmasstransfer.2021.105279.

Miansari M., Darvishi M.R., Toghraie D., Barnoon P., Shirzad H., Alizadeh A., 2022. Numerical investigation of grooves effects on the thermal performance of helically grooved shell and coil pipe heat exchanger. *Chinese Journal of Chemical Engineering*, 44(4): 424–434. DOI: 10.1016/j.cjche.2021.05.038.

Naphon P., 2007. Thermal performance and pressure drop of the helical-coil heat exchangers with and without helically crimped fins. *International Communications in Heat and Mass Transfer*, 34(3): 321–330. DOI: 10.1016/j.icheatmasstransfer.2006.11.009.

Nemati M., Sefid M., 2022. Using active/passive methods to control of MHD conjugate heat transfer of power-law fluids: a numerical entropy analysis by LBM. *International Journal of Energy and Environmental Engineering*, 14(4): 719–741. DOI: 10.1007/s40095-022-00545-x

Nitturi L.K., Kapu V.K.S., Gugulothu R., 2023. Augmentation of heat transfer through passive techniques. *Heat Transfer*, 52(5): 44222. DOI: 10.1002/htj.22877.

Panahi D., Zamzamian K., 2017. Heat transfer enhancement of shell-and-coiled pipe heat exchanger utilizing helical wire turbulator. *Applied Thermal Engineering*, 115: 607–615.

Rashidi M.M., Mahariq I., Nazari M.A., Accouche O., Bhatti M.M., 2022. Comprehensive review on exergy analysis of shell and pipe heat exchangers. *Journal of Thermal Analysis and Calorimetry*, 147(14): 12301–12311. DOI: 10.1007/s10973-022-11478-2.

Shomansurov F.F, Auesbaev A.U., Ismaylov O.Y., Khurmamatov A.M., Khametov Z.M., Muminov J.A., 2024. Optimization of the process of heating an oil and gas condensate mixture by light naphtha vapor in heat – exchanger condenser 10E04. *Nafta-Gaz*, 8: 501–510. DOI: 10.18668/NG.2024.08.05

Solanki A.K., Kumar R., 2019. Two-phase flow condensation heat transfer characteristic of R-600a inside the horizontal smooth and dimpled helical coiled pipe in shell type heat exchanger. *International Journal of Refrigeration*, 107: 155–164. DOI: 10.1016/j.ijrefrig.2019.07.017.

Tuncer A.D., Sözen A., Khanlari A., Gürbüz E.Y., Variyenli H.I., 2021. Analysis of thermal performance of an improved shell and helically coiled heat exchanger. *Applied Thermal Engineering*, 184(1): 116272. DOI: 10.1016/j.applthermaleng.2020.116272.

Yeasmin S., Billah M.M., Molla M.Z., Hoque K.E., 2022. Numerical analysis of unsteady mixed convection heat transfer characteristics of nanofluids confined within a porous lid-driven L-shaped cavity. *International Journal of Thermofluids*, 16: 100218, DOI: 10.1016/J.IJFT.2022.100218.

Zheng H., Price R.E., Modarres-Sadeghi Y., Triantafyllou M.S., 2014. On fatigue damage of long flexible cylinders due to the higher harmonic force components and chaotic vortex-induced vibrations. *Ocean Engineering*, 88: 318–329. DOI: 10.1016/j.oceaneng.2014.06.041.

Zolfagharnasab M.H., Pedram M.Z., Hoseinzadeh S., Vafai K., 2022. Application of Porous-Embedded shell and pipe heat exchangers for the Waste heat Recovery Systems. *Applied Thermal Engineering*, 211: 118452. DOI: 10.1016/j.applthermaleng.2022.118452.

Abdugaffor Mirzaabdullaevich KHURMAMATOV, Sc.D.
Head of laboratory at the Institute of General and Inorganic Chemistry
Academy of Sciences of the Republic of Uzbekistan
77a Mirzo Ulugbek Ave., 100170 Tashkent, Uzbekistan
E-mail: *gafuri_19805@mail.ru*

Ganisher Bakhtiyorovich RAKHIMOV, Ph.D.
Associate professor at the Department of Oil and Gas
Karshi Engineering-Economic Institute, Uzbekistan
Mustakillik Str., 225, 180100 Karshi, Uzbekistan
E-mail: *ganisher.raximov1@inbox.ru*

Oybek Yuliboyevich ISMAILOV, Sc.D.
Leading researcher at the Institute of General and Inorganic Chemistry
Academy of Sciences of the Republic of Uzbekistan
77a Mirzo Ulugbek Ave., 100170 Tashkent, Uzbekistan
E-mail: *ismoilovnmpi@mail.ru*

Jalolidin Azizjon MUMINOV, Ph.D.
Associate professor at the Department of Technological Machines and Equipment
Fergana Polytechnic Institute
86 Fergana Str., 150107 Fergana, Uzbekistan
E-mail: *mominovjacadem@gmail.com*

Alisher Usnatdinovich AUESBAEV, Ph.D.
Associate professor at the Karakhalpak State University named after Berdakh
1 Abdirov Str., 230112 Nukus city, Uzbekistan;
Doctoral Student at the Institute of General and Inorganic Chemistry
Academy of Sciences of the Republic of Uzbekistan
77a Mirzo Ulugbek Ave., 100170 Tashkent, Uzbekistan
E-mail: *alisherauesbaev@gmail.com*

Zamirbek Mukhtorovich KHAMETOV, Ph.D.
Head of the Department of Land Transport Vehicles and their Exploitation
Fergana Polytechnic Institute
86 Fergana Str., 150107 Fergana, Uzbekistan
E-mail: *zamir311384@mail.ru*